Society For Biomaterials

Neurotrophin-3 released from implant of tissue-engineered fibroin scaffolds inhibits inflammation, enhances nerve fiber regeneration, and improves motor function in canine spinal cord injury

Ge Li,[1]* Ming-Tian Che,[1]* Xiang Zeng,[1] Xue-Cheng Qiu,[1] Bo Feng,[1] Bi-Qin Lai,[1] Hui-Yong Shen,[2,3] Eng-Ang Ling,[4] Yuan-Shan Zeng [1,2,5,6,7]

[1]Key Laboratory for Stem Cells and Tissue Engineering (Sun Yat-sen University), Ministry of Education, Guangzhou, 510080, China
[2]Institute of Spinal Cord Injury, Sun Yat-sen University, Guangzhou, 510120, China
[3]Department of Orthopedics, Sun Yat-sen Memorial Hospital, Sun Yat-sen University, Guangzhou, 510120, China
[4]Department of Anatomy, Yong Loo Lin School of Medicine, National University of Singapore, Singapore, 117594, Singapore
[5]Department of Histology and Embryology, Zhongshan School of Medicine, Sun Yat-sen University, Guangzhou, 510080, China
[6]Co-innovation Center of Neuroregeneration, Nantong University, Nantong, 226001, China
[7]Guangdong Provincial Key Laboratory of Brain Function and Disease, Zhongshan School of Medicine, Sun Yat-sen University, Guangzhou, 510080, China

Received 4 December 2017; revised 3 March 2018; accepted 21 March 2018
Published online 25 April 2018 in Wiley Online Library (wileyonlinelibrary.com). DOI: 10.1002/jbm.a.36414

Abstract: Spinal cord injury (SCI) normally results in cell death, scarring, cavitation, inhibitory molecules release, etc., which are regarded as a huge obstacle to reconnect the injured neuronal circuits because of the lack of effective stimulus. In this study, a functional gelatin sponge scaffold was used to inhibit local inflammation, enhance nerve fiber regeneration, and improve neural conduction in the canine. This scaffold had good porosity and modified with neurotrophin-3 (NT-3)/fibroin complex, which showed sustained release *in vitro*. After the scaffold was transplanted into canine spinal cord hemisection model, hindlimb movement, and neural conduction were improved evidently. Migrating host cells, newly formed neurons with associated synaptic structures together with functional blood vessels with intact endothelium in the regenerating tissue were identified. Taken together, the results demonstrated that using bioactive scaffold could establish effective microenvironment stimuli for endogenous regeneration, providing a potential and practical strategy for treatment of spinal cord injury. J Biomed Mater Res Part A: 106A: 2158–2170, 2018.

Key Words: neurotrophin-3, controlled artificial release system, inflammation, nerve fiber regeneration, spinal cord injury

How to cite this article: Li G, Che M-T, Zeng X, Qiu X-C, Feng B, Lai B-Q, Shen H-Y, Ling E-A, Zeng Y-S. 2018. Neurotrophin-3 released from implant of tissue-engineered fibroin scaffolds inhibits inflammation, enhances nerve fiber regeneration, and improves motor function in canine spinal cord injury. J Biomed Mater Res Part A 2018:106A:2158–2170.

INTRODUCTION

Spinal cord injury (SCI) is a devastating disease of the central nervous system (CNS) resulting in partial or a complete loss of central control of neural function, leaving permanent damage to the motor, sensory, and autonomic functions below the injury site.[1] It has been widely accepted that a major challenge in recovery after SCI is to rebuild the lost neural connectivity in terms of cytoarchitecture and also function.[2,3] In line with this principle, many studies have adopted tissue engineering strategy utilizing biomaterials, such as hydrogel,[4] poly-lactic-*co*-glycolicacid (PLGA) multiple-channel conduits,[5] microspheres,[6] microparticle,[7] and so forth as the bridging materials for endogenous regeneration. However, because of the hostile microenvironment presenting persistently in the injury site of spinal cord,[8,9] very few of the attempts have succeeded in significant nerve fiber regeneration across and beyond the injury epicenter, rendering only a modest functional regain after injury. In view of this, bioactive materials

Additional Supporting Information may be found in the online version of this article.
*These authors contributed equally to this manuscript.
Correspondence to: Y.-S. Zeng; e-mail: zengysh@mail.sysu.edu.cn
Contract grant sponsor: National Key R&D Program of China; contract grant number: 2017YFA0104704
Contract grant sponsor: National Natural Science Foundation of China; contract grant numbers: 81330028, U1301223
Contract grant sponsor: Science Foundation of Ministry of Education of China; contract grant number: 201300193035
Contract grant sponsor: Science Foundation of Guangdong Province; contract grant number: 2017B020210012
Contract grant sponsor: Co-innovation Science Foundation of Guangzhou City; contract grant numbers: 201508020215, 201704020221

endowed with the capabilities of altering the adverse microenvironment of the injury site has been considered as a more promising therapeutic approach in treating SCI.

Neurotrophin-3 (NT-3) and its high-affinity receptor (tyrosine kinase receptor C, TrkC) play extensive trophic roles in neural stem cell migration, neuronal differentiation, nerve fiber (axon) outgrowth, and synapse development and plasticity in the nervous system.[10] Schwann cells overexpressing NT-3 could provide sufficient nutrition for constituting an adult stem cell-derived neural network *in vitro*.[11] This had prompted us to design a novel bioactive scaffold for the delivery of NT-3 by using the NT-3/fibroin particles as surface decoration. The gelatin sponge (NF-GS) scaffold coated with NT-3/fibroin particles had achieved a controlled artificial release system, thus providing significant therapeutic effects on nerve fiber regeneration and inflammatory inhibition in the rat SCI model.[12] The functional recovery after SCI maybe dependent on several factors: (1) Attenuation of physical (such as cavities[13]) and biochemical (such as glial scars[14] and inflammatory cytokines/cells[15]) barriers in the microenvironment, (2) Cytoarchitecture reshaping with functional neurogenesis, synaptogenesis, angiogenesis and remyelination at the injury site[16,17] and (3) Motor function restoration as manifested by improved electrophysiological recording[18] and locomotion performance. Thus, the rodent models had provided the first line evaluation of methodologies in screening potential therapeutic treatment for SCI. However, because of interspecies variation in terms of anatomy, physiology and pathophysiology, large animal models such as canine or monkey are desirable so as to comprehensively analyze the above-mentioned conditions[18] for more reliable pre-clinical conclusions.

Our study had demonstrated that NF-GS scaffold was nontoxic and could exert excellent histocompatibility in the spinal cord of rats and canines. These histopathological findings had indicated that the safe bioactive scaffold may serve as a promising biomaterial for SCI repair. This method for the treatment of spinal cord injury obviated the risk of insecurity by gene transfer techniques and of uncertain survival by cell transplantation. More importantly, it showed regeneration of functional neuronal axons, reduction of cavity formation, and remyelination of rats through the scaffold transplantation.[12] However, there was still lack of a concrete electrophysiological evidence to prove whether the bioactive scaffold plays a critical role as nutrient enrichment region to enhance endogenous regeneration. To avoid above limitations, it is highly desirable to extend the investigation by various techniques and using a larger pool of canines to determine whether bioactive scaffold would decrease inflammation of local microenvironment, and whether the favorable niche would effectively attract cells migration and functional axonal regeneration. Additionally, it is demanded to elucidate whether the cells migration and tissue regeneration could restore functional neurotransmission from brain to hindlimbs.

MATERIALS AND METHODS

NF-GS scaffold preparation

The methods for the preparation of NF-GS scaffolds have been described in detail in our previous study.[12] Briefly, sterile gelatin sponge (GS) scaffolds were tailored into a "D" shape tube with a diameter of 2 mm and a length of 4 mm, submerged in NT-3/fibroin (NF) particle solution completely and wrapped up with poly-lactic-*co*-glycolicacid (PLGA) tubes. The scaffolds used in the present experiment comprised three groups *in vitro*; (1) GS coated with NT-3/fibroin complex group [the NF-GS group, Fig. 1(A)], (2) GS coated with fibroin group [the F-GS group, Fig. 1(B)] and (3) GS without NT-3 and/or fibroin coating [the GS group, Fig. 1(C)], and two groups *in vivo*; (1) GS coated with NT-3/fibroin complex group (the NF-GS group), and (2) GS coated with fibroin group (the F-GS group or the control group).

Spinal cord injury model and transplantation

Ethics. All animal experiments were approved by the Institutional Animal Care and Use Committee (IACUC) of Sun Yat-sen University and performed in accordance with the National Institutes of Health Guide for the Care and Use of Laboratory Animals.

Experimental animals, surgery, and scaffold graft. Beagle canines (female, 7-month-old, $n = 14$), supplied by Guangzhou General Pharmaceutical Research Institute Co., Ltd, were anesthetized with 1% pentobarbital sodium (45 mg/kg, i.p.). After full anesthesia was achieved, the T9 and T10 spinal cord segments of the canines were exposed. A 4-mm segment of the spinal cord (right side) at T10 level was removed to create a hemisection model [Fig. 2(A,B,b,C,D)]. After hemostasis, the NF-GS and F-GS scaffolds were transplanted, respectively, to fill up the gap of hemisected spinal cord in the NF-GS and F-GS groups. Animals were housed in the animal facility with suitable ambient temperature and humidity. Standardized post-operative care procedures were in line with the literature for induced canine SCI model[19,20] with minor modifications and were pre-approved and supervised by the IACUC. Antibiotics and glucose dissolved in lactated ringers solution was intravenously delivered for 3 days. Dysfunction of micturition reflex was transient and their bladders were manually emptied three times a day until autonomic bladder function was restored (usually within 7 days).

Scanning electron microscopy

The scaffolds in different groups were examined by scanning electron microscopy (SEM). They were fixed in 4% paraformaldehyde for 20 min, washed three times with PBS, stored overnight at −80°C, and freeze-dried for 12 h. The dried samples were coated with gold and examined under a scanning electron microscope (Philips XL30 FEG).

Immunoelectron microscopy

The NT-3 bioactivity of scaffolds in different groups was examined with immunoelectron microscopy (IEM). Scaffolds were fixed with stationary liquid (0.1*M* PB, 4% PFA, 0.1% glutaraldehyde and saturated picric acid) for 30 min, washed three times with PB, and then transferred into cryoprotectant solution (0.1*M* PBS, 25% sucrose, and 10% glycerol) for 1 h, and followed by a quick freeze-thaw in liquid

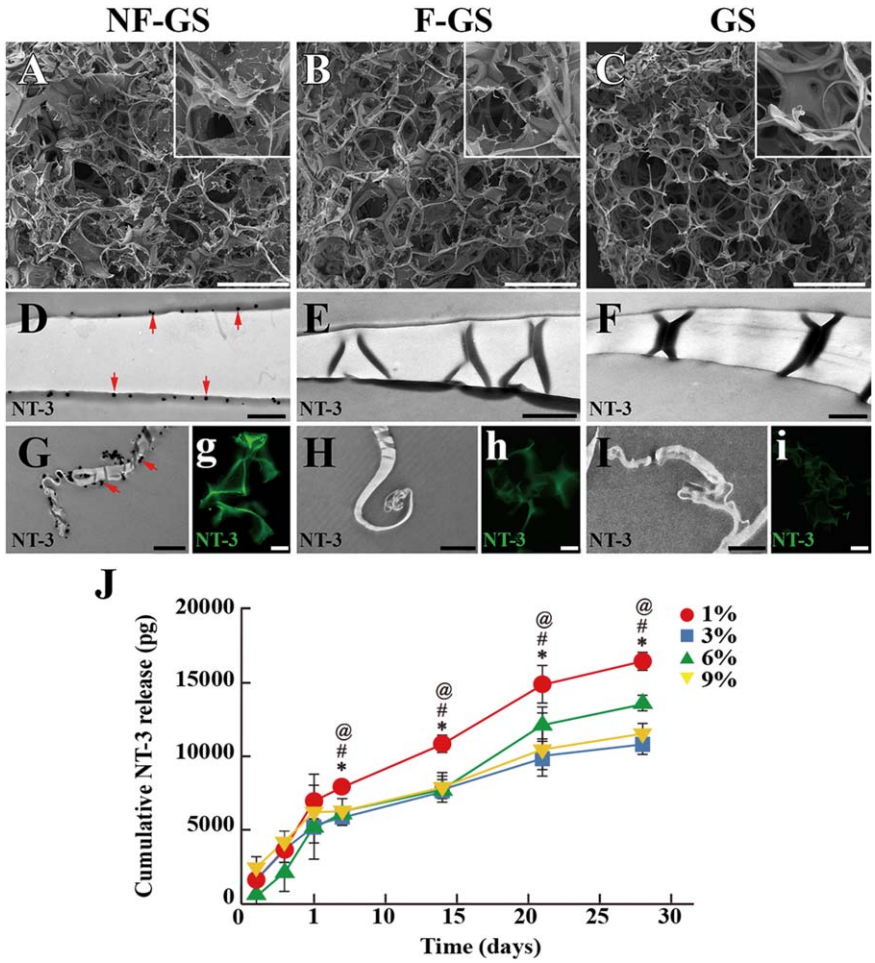

FIGURE 1. Structural features and bioactivity of the scaffold. Showing NF-GS (A), F-GS (B), and GS (C) with porous microstructure at low magnification. D: Showing NT-3 positive sites (red arrows) on NF-GS were labeled by gold enhanced nanogold particles. NT-3 positive sites are absent in F-GS (E) and GS (F). G: Showing NT-3 positive gold enhanced nanogold particles (red arrows) on the surface of random coil structure of NF-GS. (g) Showing NT-3 positive sites on the surface of NF-GS by immunofluorescence staining. NT-3 positive particles are absent on the surface of random coil structure of F-GS (H) and GS (I). NT-3 positive sites are absent on the surface of F-GS (h) and GS (i) by immunofluorescence staining. J: Cumulative release profile of bioactive NT-3 from NF-GS of different fibroin concentrations up to 28 d. $n = 5$, $^{*}p < 0.05$, $^{\#}p < 0.05$, $^{@}p < 0.05$. Scale bars = 500 μm in (A–C); 125 μm in (a–c); 500 nm in (D–I); 20 μm in (g–i).

nitrogen. Each sample was washed with PBS and treated with 20% goat serum for 40 min to block antibody nonspecific binding. Samples were incubated firstly with NT-3 antibody (Rabbit) with 2% goat serum at 4°C for 24 h, and then with gold-anti-rabbit antibody overnight at 4°C, and postfixed in 1% glutaraldehyde for 10 min. The samples were detected by gold enhanced with GoldEnhance™ kit (NanoProbe, Yaphank, NY), osmicated, dehydrated, and embedded in Epon812. Epon812 blocks were sectioned, and ultrathin sections were prepared and examined under an electron microscope (Philips CM 10, Eindhoven, Holland).

Enzyme-linked immunosorbent assay

The NT-3 release from NF-GS with different fibroin concentrations was examined by enzyme-linked immunosorbent assay (ELISA). The gelatin sponge was cut into 2 × 2 × 2 mm^3, soaked in 200 ng/mL NT-3 with 1%, 3%, 6%, and 9% fibroin, respectively. The different NF-GS samples were incubated with PBS at 37°C, and PBS was changed at 1, 3, 5, 7, 14, 21 and 28 d to collect the supernatant. NT-3 in the supernatants was detected using commercial enzyme-linked immunosorbent assay (ELISA) kits (Boster, Wuhan, China) following the instructions of the manufacturer's protocol.

Functional recovery and locomotion performance assessment

Olby score test was carried out for the canines before and weekly after SCI surgery.[21] Briefly, the canines were trained to freely walk through the recording area where a high speed video recording camera was equipped. Multiple gait parameters such as hindlimb stepping, body weight support, accurate plantar placement of the paw, forelimb and hindlimb coordination, and trunk stability were analyzed after recording. The relative position of the hip, the knee, and the ankle joint was visualized by the black line which showed the leg ipsilateral to the hemisection, and the blue line showing the contralateral leg [Fig. 3(A,B)]. Olby score is a 15 points scoring scale that is rating based on the canine's

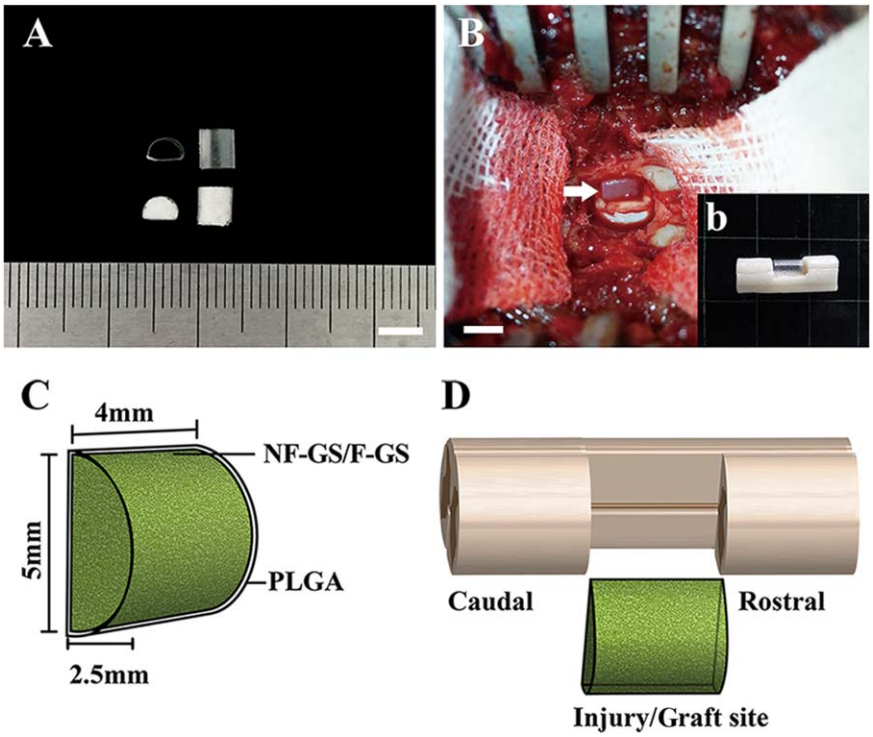

FIGURE 2. Scaffold preparation and transplantation. A: Showing two PLGA tubes (top) with a semi-diameter of 2.5 mm and two gelatin sponge D-shaped scaffolds (bottom). B: Showing a scaffold transplanted into the hemisection site (arrow, b) of spinal cord. C: Schematic diagram of a scaffold. D: grafted a scaffold in the hemisection site of spinal cord. Scale bars = 5 mm in (A) and (B).

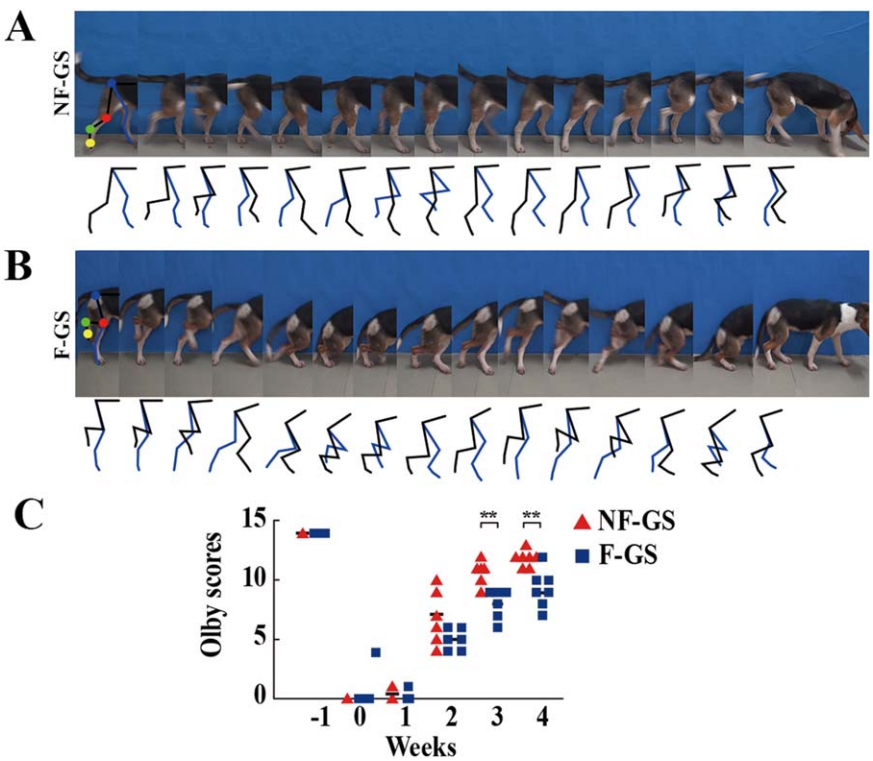

FIGURE 3. Examination of hindlimb movement and assessment of Olby score. Continuous time-lapse frames from video displayed two hindlimbs (black line representing the leg of the hemisection side of spinal cord and blue line representing the leg of the non-hemisection side) motioning alternately, involving four major joints; hips (blue point), knees (red point), ankles (green point) and digits (yellow point), in a canine of the NF-GS (A) and F-GS group (B). The stepping trajectories in (A) and (B) show respectively the relative position of the four major joints during the hindlimb movement. C: Showing Olby scores in the NF-GS and F-GS groups. $n = 7$, $^{*}p < 0.05$, $^{**}p < 0.01$.

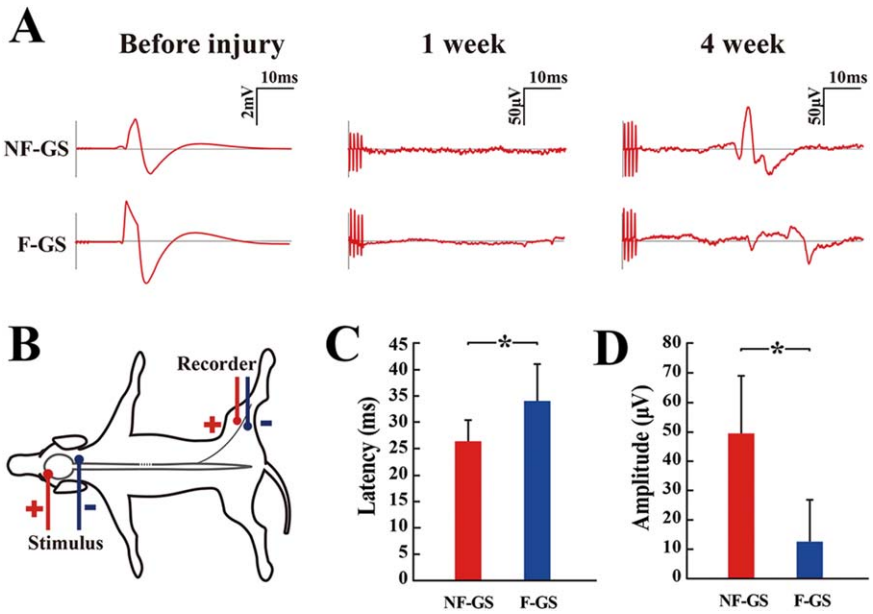

FIGURE 4. Examination of cortical motor evoked potentials (CMEP). A: CMEPs in the NF-GS (upper curves) and F-GS (lower curves) groups were respectively recorded by electrophysiological analysis before spinal cord injury, at 1 week and 4 weeks after the transplantation. B: A leading diagram showing evaluation of CMEP. Left panel: stimulus points in head; Right panel: recorder points in the leg of the hemisection site. C: Bar chart showing latency of CMEPs of two groups of canines at 4 weeks after scaffold transplantation ($n = 4$, $^*p < 0.05$). D: Bar chart showing amplitude of two groups at 4 weeks after transplantation ($n = 4$, $^*p < 0.05$).

limb movement including activities, deep pain in the hindlimbs, joints and weight bearing corresponds.[21] The Olby score for each animal was calculated weekly by averaging the independent scores from two investigators who monitored the videotapes with a double-blinded study design.

Cortical motor evoked potentials

Four weeks after graft implantation, canines ($n = 4$ in the NF-GS group and $n = 4$ in the F-GS group) were atropinized (0.5 mg/canine, intramuscular injection, 20 min before surgery), anesthetized with pentobarbital sodium (3% dissolved in saline, 45 mg/kg, intraperitoneal injection) and ketamine (10 mg/kg, intramuscular injection every 20 min during surgery), and fixed on a stereotaxic frame. The sciatic nerve and sensorimotor cortex (SMC) were exposed; a stimulation electrode was then connected to the SMC and a recording electrode was coupled to the sciatic nerve [Fig. 4(B)]. The cortical motor evoked potentials (CMEP) were detected by NeuroExam M-800 (Medcom Technology, Zhuhai, China). The stimulation protocol of the CMEP signal was as follows: gain parameter 250, time constant 150 μs, and pulse width 100 mA. To elicit a CMEP, multiple-pulse-stimulation was transmitted through the electrodes, with an interval of 1000 μs for 4 times. In order to obtain high-quality waveforms for the CMEP signals, 40 CMEP responses were averaged for each canine.

Immunofluorescence staining

Spinal cord tissue sections of 25 μm thickness were cut using a cryostat ($n = 7$ in the NF-GS group and $n = 7$ in the F-GS group). The sections were incubated with primary antibodies (Rabbit-IBA-1, Rabbit-NF, Mouse-GFAP, Rabbit-NT-3 or Mouse-MBP diluted in 0.3% Triton X-100 PBS), respectively, overnight at 4°C, followed by incubation with secondary antibodies (goat origin with Cy3 or FITC conjugated), respectively. A summary of above antibodies is provided in Table 1. The slides were then examined under a confocal fluorescence microscope (Zeiss, Oberkochen, Germany).

A total of 10 tissue sections derived from every fifth horizontal section containing T8-T12 segments (approximately 10 mm) of each spinal cord were selected from each animal. The sections were photographed after immunofluorescence staining. Eight 0.7 × 0.5 mm^2 areas covering the rostral and caudal areas to/in the injury/graft site of each the horizontal section were chosen for closer analysis [Fig. 5(A)]. The positive-stained area of NF or GFAP was converted to an area of interest (AOI) and the pixel area for each AOI was automatically calculated using Image-Pro Plus software (Media Cybernetics, Silver Spring, MD). The relative density of NF and GFAP positive staining for each image was represented by the ratio of the total pixels of AOI to the total pixels of the field.

Transmission electron microscopy

The spinal cord was fixed in 4% paraformaldehyde, and cut into 100 μm thick horizontal sections with a vibratome. The sections were washed with PBS for three times and further fixed in paraformaldehyde for 4 h. Each tissue section was placed in PBS overnight at 4°C, and subsequently fixed with 1% osmic acid for 2 h, and then dehydrated through a graded series of alcohol (50%–100%). The sections containing the injury/graft site of spinal cord were embedded in Epon812 at 60°C for 48 h. Ultrathin sections were cut with an ultramicrotome (Reichert E, Co., Vienna, Austria).

TABLE 1. Primary and Secondary Antibodies

Antibodies	Species	Type	Dilution	Source
Ionized calcium-binding adapter molecule 1 (IBA-1)	Rabbit	Monoclonal IgG	1:300	Wako, Japan
Neurofilament 200 (NF)	Rabbit	Polyclonal IgG	1:500	Merck Millipore, Billerica, USA
Glial fibrillary acidic protein (GFAP)	Mouse	Monoclonal IgG	1:300	Sigma, St. Louis, USA
Myelin basic protein (MBP)	Mouse	Monoclonal IgG	1:500	Merck Millipore, Billerica, USA
Neurotrphin 3 (NT-3)	Rabbit	Polycolonal IgG	1:300	Sigma, USA
Cy3 conjuncted anti rabbit secondary antibody	Goat	Polyclonal IgG	1:600	Jackson ImmunoResearch, West Grove, USA
FITC conjuncted anti mouse secondary antibody	Goat	Polyclonal IgG	1:50	Jackson ImmunoResearch, West Grove, USA

Following staining with lead citrate and uranyl acetate, the sections were examined under a Philips CM10 electron microscope (Eindhoven, Holland).

Statistical analysis

Data were presented as means ± standard deviations (SD). All statistical analyses were performed using the statistical

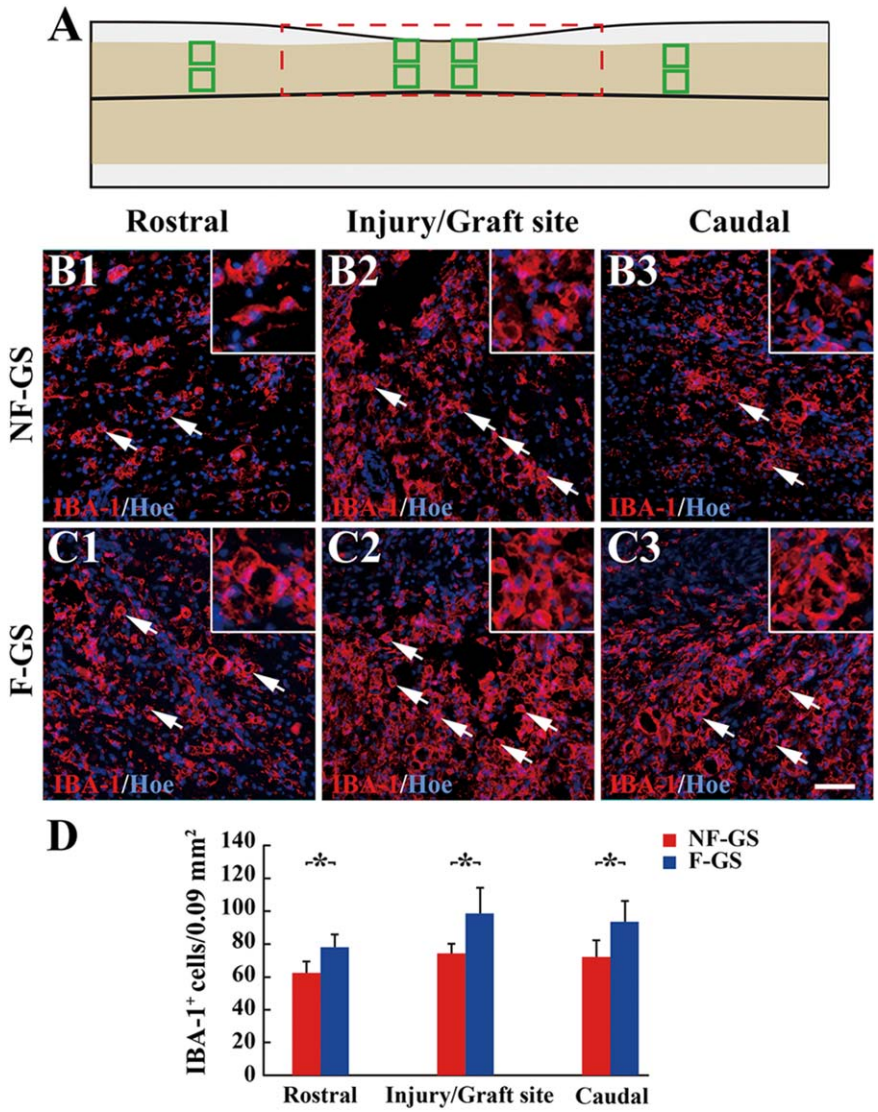

FIGURE 5. IBA-1 positive cells in spinal cord. A: A leading diagram demonstrates cell sampling sites in a longitudinal section of hemisected spinal cord. IBA-1 positive cells (arrows) in the rostral (B1), injury/graft (B2), and caudal (B3) sites of spinal cord in the NF-GS group. IBA-1 positive cells (arrows) in the rostral (C1), injury/graft C2) and caudal (C3) sites in the F-GS group. D: Bar chart showing the number of IBA-1 positive cells in the NF-GS and F-GS groups. Asterisks indicate statistical significance between the NF-GS and F-GS groups. All nuclei of IBA-1 positive cells were counterstained by Hoechst33342 (Hoe); $n = 5$, $^*p < 0.05$. Scale bar = 50 μm in (B1–C3)

software SPSS11.0. Two-group comparisons were tested by independent *t*-test or Wilcoxon. A statistically significant difference was accepted at $p < 0.05$.

RESULTS

Structural features and bioactivity of the scaffold

SEM images showed that NF-GS, F-GS and GS scaffolds contained multiporous structure, conducive for cell adhesion, nutrition, and oxygen exchange [Fig. 1(A–C)]. After NT-3/fibroin or fibroin coating, NF-GS or F-GS exhibited many crystal-like structures on the surface when compared with the GS. IEM was used to reveal the crystal-like structures. Specifically, NT-3 positive gold enhanced nanogold particles were located on the smooth [Fig. 1(D)] and random coil surface [Fig. 1(G)] of NF-GS. Nanogold particles were not detected on the smooth or random coil surface in the F-GS nor the GS scaffolds [Fig. 1(E,F,H–I)]. The localization of NT-3 was confirmed by comparing this with the immunofluorescence labeling [Fig. 1(g–i)]. To determine the optimum concentration of fibroin, the bioactivity of NT-3 released from NF-GS was tested. During the test period, 1% fibroin showed the highest level and stable cumulative NT-3 release at 7, 14, 21, and 28 d, while the other concentrations showed a lower level NT-3 release [Fig. 1(J)]. The results suggest that NF-GS combined with 1% fibroin release a more substantial bioactive NT-3 over a long duration up to 28 days.

Scaffold preparation

PLGA film (0.02 mm thick) was prepared in a "D" shaped tube of 4 mm in length and 2.5 mm in radius [Fig. 2(A), top]. Gelatin sponge containing NT-3/fibroin complex was tailored into the same shape followed by stuffing it into the "D" shaped PLGA tube [Fig. 2(A), bottom]. PLGA tube served to confine the NT-3/fibroin gelatin sponge within it and help maintain the scaffold geometry during implantation procedure. After a hemisection of spinal cord was made, the NF-GS or F-GS scaffolds were respectively placed into the ipsilateral side (right side) of the severed spinal cord [Fig. 2(B,b)]. The schematic diagrams in Figure 2(C,D) show the preparation of the "D" shaped scaffolds [Fig. 2(C)] and the implantation of a scaffold in the hemisected spinal cord [Fig. 2(D)].

Improvement of locomotor function with NF-GS

Continuous time-lapse frames derived from the high-speed videotaping were extracted to show the coordination of the hindlimbs and the involvement of four major joints (the hips, the knees, the ankles, and the digits) when initiating movement [Fig. 3(A,B)]. Coordination between two hindlimbs was closely monitored and observed by the stepping trajectory [Fig. 3(A,B)]. Thus, hindlimb voluntary movement as well as plantar placement was evidently improved in the NF-GS group of canines. In contrast, canines in the F-GS group struggled to walk on the ground with their forelimbs while their hindlimbs were walking passively with non-weight bearing. To evaluate quantitatively the functional improvements, Olby score concerning hindlimb locomotion was obtained [Fig. 3(C)]. The Olby scores of canines were significantly higher in the NF-GS group than that in the F-GS group throughout the entire course of recovery. The mean of scores was 11.85 ± 0.64 in the NF-GS group and was 9.29 ± 1.48 in the F-GS group for 4 weeks after transplantation.

Cortical motor evoked potentials

To further assess the functional status of the hemisected spinal cord injury, the cortical motor evoked potentials (CMEP) were additionally measured following transplantation treatment. As a widely used clinical evaluation, the peak and width of CMEP are interpreted conventionally as major parameters reflecting the number of excited nerve fibers and their conduction velocity of the nerve, respectively. In the group treated with NF-GS scaffold implantation, there were shortened latency and increased amplitude of CMEP [Fig. 4(A,C,D)]. Canines in the F-GS group showed negligible signal level of CMEP, which were in sharp contrast with those of the NF-GS group. The results suggest that there is likely a neuronal circuit to conduct signal from the supraspinal descending pathways, such as corticospinal or rubrospinal pathway.

Inflammation

Injury to the spinal cord results in inflammatory reaction characterized by accumulation of massive IBA-1 immunoreactive macrophages/microglia. At 4 weeks after spinal cord hemisection, IBA-1 positive cells were found in the injury/graft site and its neighboring gray matter of the spinal cord (Fig. 5). Immunofluorescence staining results showed that there were relatively fewer IBA-1 positive cells [Fig. 5(B2,D), 74.11 ± 5.85 cells/0.09 mm^2] in the injury/graft site in the NF-GS group, compared with that [Fig. 5(C2,D), 98.41 ± 15.43 cells/0.09 mm^2] in the F-GS group ($n = 5$ in each group; $*p < 0.05$). There were lesser IBA-1 positive cells (rostral, 62.43 ± 6.78 cells/0.09 mm^2 and caudal, 72.05 ± 9.33 cells/0.09 mm^2) in host tissue areas to the injury/graft site of spinal cord in the experimental group than that (rostral, 78.00 ± 7.29 cells/0.09 mm^2 and caudal, 92.75 ± 12.62 cells/0.09 mm^2) in the F-GS group [Fig. 5(B1,B3,C1,C3,D), $n = 5$ in each group, $*p < 0.05$]. Consequently, the results suggest that NT-3 delivery only induces lower immunogenicity and that NT-3 delivery scaffold has better biocompatibility with the normal spinal cord tissue.

Nerve fiber regeneration and glial scar

In both the NF-GS and F-GS groups, the injured spinal cord showed a noticeable macroscopic structural repair at the hemisected sites (Supporting Information Fig. 1), but apparently to a different extent. On closer examination, the NF-GS group exhibited a better host–implant integration with a more robust nerve fiber regeneration as compared with the F-GS group. Figure 6 showed the relative density of NF positive staining (equivalent to nerve fiber number) and relative density of GFAP positive staining (equivalent to glial scar area) in the experimental and control groups. Four weeks after transplantation, NF positive nerve fibers distributed

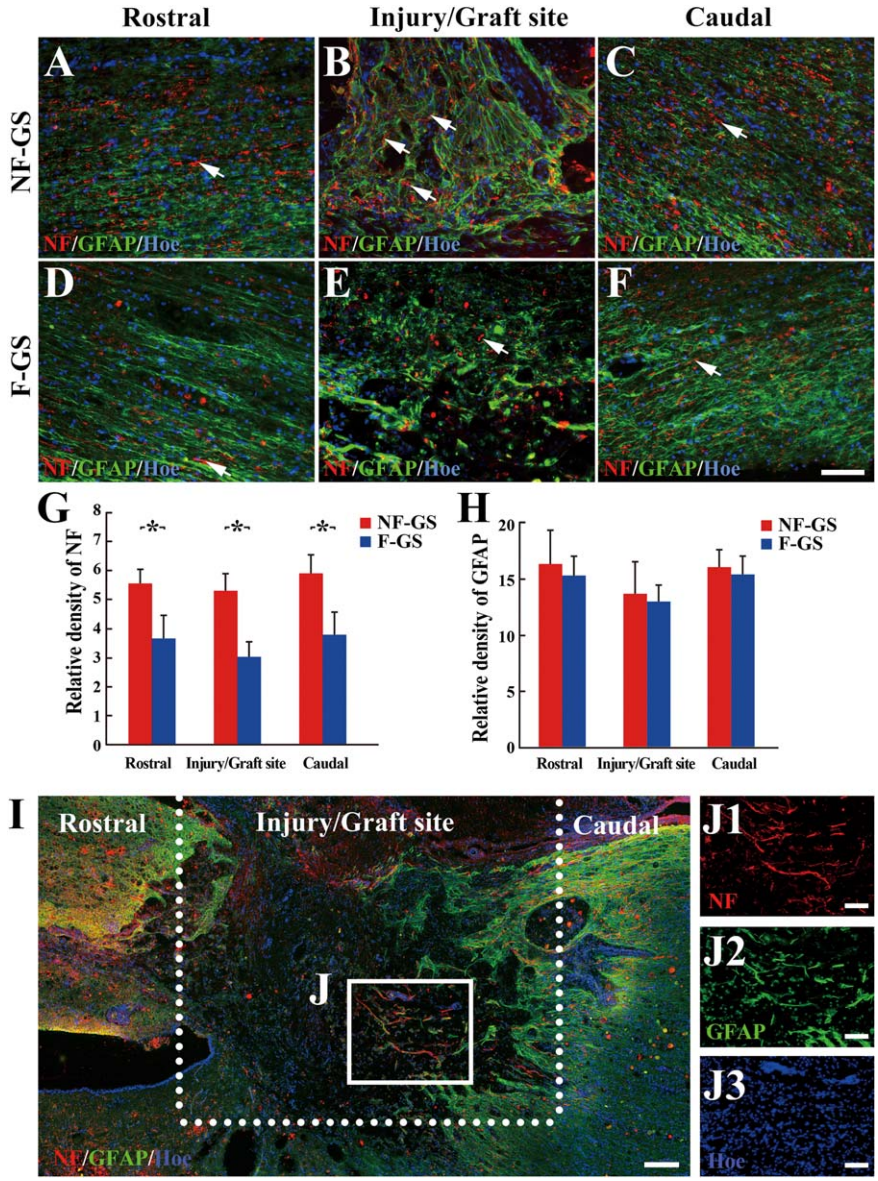

FIGURE 6. Comparison of NF positive nerve fibers and GFAP positive scars in spinal cord. NF positive nerve fibers (red, arrows) and GFAP positive scars (green) in the rostral (A), injury/graft (B), and caudal (C) sites of spinal cord in the NF-GS group. NF positive nerve fibers (red, arrows) and GFAP positive scars (green) in the rostral (D), injury/graft (E), and caudal (F) sites in the F-GS group. G: Bar chart shows the relative density of NF positive nerve fibers at the rostral and caudal to/in the injury/graft site of spinal cord in the NF-GS group was higher than that in the F-GS groups; $*p < 0.05$. H: Bar chart shows the relative density of GFAP positive scar at the rostral and caudal to/in the injury/graft site of spinal cord in the NF-GS group was comparable to that in the F-GS group; $n = 7$, $p > 0.05$. I: An overview of NF and GFAP immunofluorescence staining in a longitudinal section in the NF-GS group. J: Note host neurons extended NF positive nerve fibers (red) from the caudal sites into the injury/graft site of spinal cord. A higher magnification of boxed area (J) in (I) displaying the overlaid image of NF, GFAP, and Hoechst33342 (Hoe)-labeled objects, to demonstrate that host neurons can extend NF positive nerve fibers (J1, red) through GFAP positive scars (J2, green), (J3, blue). Nuclei of cells in the injury/graft site were counterstained by Hoe. Scale bars = 200 μm in (I); 100 μm in (A–F) and (J1–J3).

from rostral to caudal area of spinal cord in two groups [Fig. 6(A–F)]. The relative density of NF positive nerve fibers in the rostral and caudal to/in the injury/graft site ($5.55 \pm 0.49\%$, $5.31 \pm 0.55\%$ and $5.89 \pm 0.64\%$) in the NF-GS group is higher than that ($3.67 \pm 0.77\%$, $3.05 \pm 0.49\%$ and $3.80 \pm 0.78\%$) in the F-GS group [Fig. 6(G), $n = 7$ in each group, $*p < 0.05$]. However, the relative density of GFAP positive glial scars from rostral to caudal area between the NF-GS ($16.21 \pm 2.98\%$, $13.58 \pm 2.84\%$ and $15.92 \pm 1.38\%$) and F-GS ($15.62 \pm 1.62\%$, $12.97 \pm 1.45\%$ and $15.25 \pm 1.76\%$) groups was not significantly different [Fig. 6(H), $n = 7$ in each group, $p > 0.05$]. NF positive nerve fibers were evident in the injury/graft site of spinal cord in the NF-GS group [Fig. 6(B,J1)]. The regenerating nerve fibers appeared to traverse the glial scar site and penetrated the graft area of spinal cord in the experimental group [Fig. 6(A–C,J,J2)]. That the regenerating nerve fibers extended over a long distance in the graft area of spinal cord suggests

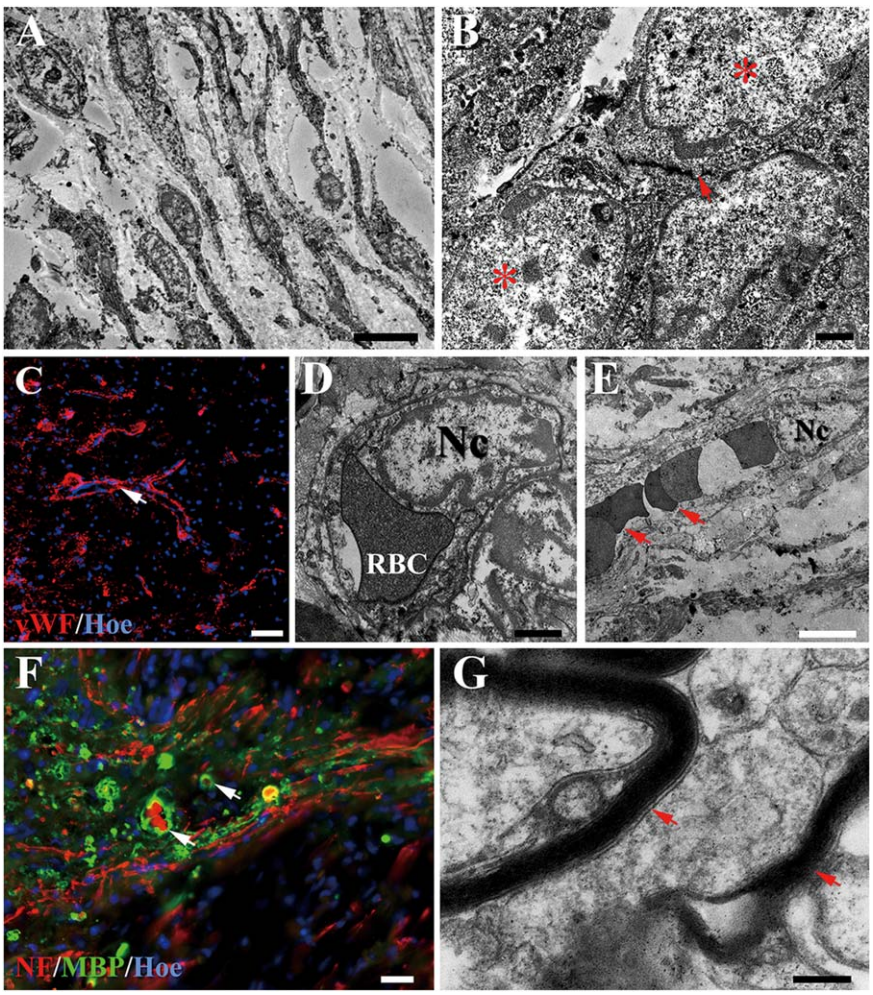

FIGURE 7. Cell migration and revascularization in the injury/graft site of spinal cord in the NF-GS group. A: TEM shows many cells appear to migrate into NF-GS implant. B: A neuron-like cell (asterisk) containing an aggregation of flattened "synaptic" vesicles (arrow) appears to make a synapse-like contact associated with another neuron-like cell (asterisk) under the electron microscopy. C: Note the presence of vascular profiles in the injury/graft site in confocal microscopy, the white arrow indicates the vascular walls. Blood capillaries in transverse (D) or longitudinal (E) section are identified by the lining endothelial cells showing an irregular nucleus (Nc). Note the endothelial cell is invested by a layer of basal lamina (D). Erythrocytes (RBC, arrows) are present in the vascular lumen (E). F, G: Some unmyelinated nerve fibers (NF positive) and a few profiles of myelinated nerve fibers (arrows) were found in the injury/graft site. Scale bars = 5 μm in (A); 2 μm in (B); 50 μm in (C) and (D); 1 μm in (E); 25 μm in (F); 1 μm in (G).

that the microenvironment of NF-GS implant was conducive for nerve fiber regrowth, and that the slow-release NT-3 may promote the nerve fiber regeneration.

Cell migration and revascularization

By electron microscopy (EM) and laser confocal microscopy, many fusiform cells appeared to infiltrate the injury/graft site of spinal cord in the NF-GS group [Fig. 7(A)]. Some of them were neuron-like cells making synapse-like contacts or junctions with the adjacent cells; a few flattened vesicles were observed in the cytoplasm on one side of the junction [Fig. 7(B)]. Blood vessels or capillaries lined by endothelial cells were identified only in the NF-GS group [Fig. 7(C–E)]. Many unmyelinated nerve fibers and nerve fibers enveloped by myelin sheath were observed. Occasional NF positive nerve fibers were wrapped by MBP positive structure in the injury/graft site at 4 weeks after the scaffold transplantation [Fig. 7(F,G)]. However, cell migration was also observed in the injury/graft sites of spinal cord in the F-GS group (Supporting Information Fig. 2). Some cells were distributed in the center of the injury/graft site (Supporting Information Fig. 2A, arrows). Glial scar appeared to form a barrier-like structure between the migration cells (Supporting Information Fig. 2A, asterisk). In addition, degenerating structures with a lamellar appearance, suggesting to be of myelin sheath nature, were observed at and around the injury/graft site (Supporting Information Fig. 2B, arrows). Vascular profiles were not encountered in the injury/graft sites in the F-GS group despite a thorough search. Taken together, the results suggest that grafted NF-GS scaffold could improve the injured microenvironment and attract cell migration into the graft area of spinal cord, and delivery of NT-3 may be a key factor in promoting the cell migration.

DISCUSSION

With the rapid growth in translational medicine, more studies using experimental large animals such as canines[22] or monkeys[23] have yielded some interesting results before preclinical trial. Transplantation of NF-GS had created a microenvironment with attenuated inflammation that is favorable for increased survival of infiltrated tissue cells and enriched re-innervation from the host neurons inside the graft. Vascularization, indicative of a successful of graft-host integration, was verified by electron microscopy, in which functional blood vessel, with intact endothelium and containing red blood cells were defined. The reconstitution of the cytoarchitecture by NF-GS graft facilitates neural conduction and motor function recovery, as evidenced by the improved CMEP and Olby score following NF-GS grafting. All these have indicated a better tissue repair together with functional regain through use of this NT-3 sustained local delivery scaffold after canine SCI.

A local immune reaction in the spinal cord following injury is elicited in rats[24] and monkeys.[25] The ensuing recruitment of inflammatory cells dominates the resources in the injury site of spinal cord rostral and caudal to the epicenter, and this can lead to progressive degeneration of neurons.[26] The adverse condition is compounded by the transplantation of cells or biodegradable materials in which degradation products and necrotic corpses are viewed by the host cells as foreign and mount an attack with more reactive microglia and phagocytic macrophages.[27] As mentioned before, inflammatory cells in acute period rapidly invaded the damaged region of the spinal cord between 3 to 7 days post-injury, suggesting an early neuroprotective response. The secondary phase of inflammation which occurs over a period of months is featured by a long-lasting contribution of immune cells to the inflammatory environment within the spinal cord after injury.[28] Therefore, immune reaction assessment is crucial for effective treatment for SCI. Typically, IBA-1 cells have prominent and ramified processes, indicating that some of them are microglia derived.[29,30] To investigate the inflammatory response, IBA-1 immunohistochemistry was carried out following NF-GS graft. The results showed that release of NT-3 mitigated the local inflammation, and the numbers of IBA-1 positive cells were significantly decreased in the NF-GS group compared with the control F-GS group. Many studies have reported time-dependent changes of inflammatory and neurotrophic process in ischemic retina[31] and multiple sclerosis.[32] However, it has remained uncertain whether there is a link between the neurotrophins and inflammatory systems. Notwithstanding, the present results suggest that NT-3 may play a positive role in suppressing inflammation; hence, use of bioactive scaffolds with anti-inflammatory cytokines is a potential therapeutic approach for SCI.

NT-3 is regarded as a classical trophic factor that plays pivotal roles in cell survival, differentiation, and axonal growth in the central nervous system.[33] It has been reported that there is an intrinsic downregulation of NT-3 in the adult mammalian spinal cord; therefore, the rationality of using NT-3 after SCI with the hope for recurrence of developmental events in the injury site, especially for axonal regrowth.[34] To initiate an early repair process, most studies involved delivery of NT-3 in or close to the SCI lesion epicenter, immediately after the injury.[35,36] Very interestingly, it would appear that even when it is delivered in the chronic phase, NT-3 exerts tissue repair efficacy. For example, transplantation of mesenchymal stem cells (MSCs) modified by NT-3 gene at 6 weeks post-injury resulted in discernible axon regeneration through scars, indicating a wider therapeutic window to be feasible.[37] Besides local delivery, stimulation of synthesis and release of endogenous NT-3 is a possible approach through electrical acupuncture method.[38,39] For a sustained local delivery strategy, we have designed a NF-GS bioactive scaffold, acting like a pump which can establish a NT-3 gradient within the injury site and create a preferable local microenvironment for pro-repairing cells. In the latter, some neuron-like cells with associated synapses and containing synaptic vesicles were identified by electron microscopy. Myelinated nerve fibers were also identified in the same area. The multilayered myelin tended to enwrap the regenerating nerve fibers which extended in different orientations. A variable number of nerve fibers were unmyelinated. Remyelination has been reported in a separate SCI study using NT-3 overexpressing transgenic Schwann cells.[40] A study using LINGO-1 antagonist showed the presence of many new myelin in lumbar spinal cord of rats[41] suggesting therefore that formation of multiple layered myelin sheath in hemisected SCI canine is possible. Interestingly, it has also been proved that remyelination occurred in a naturally-occurring SCI canine after 17 days without any treatment.[42] It is well established that myelin sheath can improve the speed of neuronal conduction. The present results showed that the CMEPs in the NF-GS group had shortened latencies suggesting a faster speed of neuronal conduction than that in the control group. A remarkable feature in this study was the occurrence of some capillaries in the injury/graft site. Furthermore, the cells in the injury/graft comprising the endothelial cells, neurons, astrocytes and oligodendrocytes expressed NT-3's high-affinity receptor TrkC.[43,44] This suggests that the migration of endogenous cells may be directly induced by the interaction of ligand and receptor.[45] Bioactive scaffold therefore provides a supportive microenvironment for cell migration.

Different experiments have been designed for testing chronic and acute changes of plasticity and motor function in injury animal models. This includes tests for functional recovery to sensorimotor system of the central nervous system after injury. The cylinder test has provided a way to evaluate a rodent's spontaneous forelimb use and has been used in a number of motor system injury models of stroke.[46] Basso, Beattie, Bresnahan locomotor rating scale (BBB) is an effective measure of locomotor functional recovery to predict anatomical variations at the lesion center for spinal cord injury, and more widely used in rats.[47] In canines, Olby score is routinely used for endpoint measurements, kinematic measurements and kinetic measurements.[21] Here, we have compared the ground forces applied by the two hindlimbs and used

force differences of gait between the limbs to estimate recovery. A similar Olby score was used in our previous study which reflected the effectiveness of the treatment for SCI.[8,12] With NT-3 delivery, canines showed excellent CMEP and coordinate limb movement. Additionally, hindquarters were supported at the tail to provide balance. There was evidence to support the NT-3-induced spinal circuitry plasticity to affect the changes necessary to promote the locomotor improvements. In a mature neuronal circuit, it is easy to establish the voluntary muscular contraction on one side of the organization by producing communication in the contralateral corticospinal motor pathway.[48–50] With four canines in each group, we tested their CMEPs, and compared them with the CMEP before injury, 1 week and 4 weeks after graft. The electrophysiological result showed that the NF-GS group presented a higher amplitude and shorter latency of CMEPs than the control group, thus supporting the behavioral performance. Formation of new local circuits and neuronal relay may be one of the most important reasons why behavioral improvement and CMEP waves were obvious in our present study. However, compared with normal canines (amplitude, 3.06 ± 0.97 mV; latency, 12.96 ± 1.00 ms), it was clearly not enough and more neuronal circuits would be desirable in a spinal cord hemisection for a further functional recovery.

Collateral axonal sprouting coming from the contralateral corticospinal tract may play a role in motor improvement.[51,52] It is speculated that increased in local NT-3 level may help axonal sprouting as well as strengthen the motor neurons (L3-S4) to the sciatic nerve. The functional change is supported by the existence of a circuit of neurons in the lumbar spinal cord called the central pattern generator(CPG).[53] It has been reported that electrical stimulation can increase the expression of NT-3 in the lumbar motor neurons and alleviate the muscle atrophy in the hindlimb, which will allow for the new treatment strategy in the injured spinal cord.[54] In accordance with our previous work,[12] we have provided here with further evidence that supports the use of bioactive scaffold to reform central pattern-generating circuitry of spinal interneurons in canines. Similar to using genetically engineered to delivery NT-3,[11] bioactive scaffolds are evidently beneficial to improve post-injury environment and to circumvent the risk of virus transmission. More importantly, this strategy has alluring prospect of clinical application for spinal cord injury. However, as observed by immunofluorescence staining, GFAP positive glial scar showed no difference in two groups, suggesting that the concentration of NT-3 used in this study did not show a significant impact on the glial scar of canines. It is now clear that glial scar is not simply an all-or-nothing phenomenon and came from reactive astrocytes.[55,56] Much less is known, unlike the periphery of the injury site in the rat spinal cord,[12] increased stiffness of GFAP positive glial scar occupied a large scale extending from the edge of lesion to the distal area of the host in canine spinal cord. It is speculated that glial scar may be enhanced from lower to higher animals.[57,58] If it is so, that would be the greatest challenge from animal experiment to clinical translation for SCI repair. Further study is needed to determine the optimal concentration of NT-3 used for big animal or human, and whether other factors along with NT-3 could be used to select suitable endogenous cells for SCI treatment in future. All in all, the scaffold we have designed is able to upregulate local NT-3 level in the injury/graft site of spinal cord, to become a bridge for the growth and contact of neurons, and to facilitate our future experiments such as loading of stem cells for repairing SCI.

CONCLUSION

The present study offered a promising therapeutic strategy by transplanting bioactive scaffold into the hemisected spinal cord of canine. The results demonstrated that NT-3 delivery from bioactive scaffold evidently inhibited the inflammatory reaction, yielded a favorable environment which promoted nerve fiber regeneration, attracted the migration of host tissue cells into the injury/graft site to form myelin sheath and blood vessels, and eventually improved the paralytic hindlimb locomotion with increased amplitude and shortened latency of cortical motor evoked potentials. Most importantly, our study provides a histomorphological and electrophysiological basis on how the bioactive scaffold may help improve the motor function in canine with hemisection SCI.

COMPETING INTERESTS

The authors declare that they have no competing interests.

AUTHOR CONTRIBUTIONS

Concept and design, YSZ; acquisition of data and experiments performance, GL, MTC, XZ, XCQ, BF, BQL, HYS; analysis and interpretation, GL, MTC, XZ, EAL, YSZ; drafting and editing of the manuscript, GL, MTC, XZ, EAL, YSZ. The manuscript was written through contributions of all authors. All authors have given approval to the final version of the manuscript.

REFERENCES

1. Dumont RJ, Okonkwo DO, Verma S, Hurlbert RJ, Boulos PT, Ellegala DB, Dumont AS. Acute spinal cord injury, part I: Pathophysiologic mechanisms. Clin Neuropharmacol 2001;24:254–264.
2. Kwon BK, Tetzlaff W, Grauer JN, Beiner J, Vaccaro AR. Pathophysiology and pharmacologic treatment of acute spinal cord injury. Spine J 2004;4:451–464.
3. Beattie MS, Farooqui AA, Bresnahan JC. Review of current evidence for apoptosis after spinal cord injury. J Neurotrauma 2000; 17:915–925.
4. Liu SW, Sandner B, Schackel T, Nicholson L, Chtarto A, Tenenbaum L, Puttagunta R, Muller R, Weidner N, Blesch A. Regulated viral BDNF delivery in combination with Schwann cells promotes axonal regeneration through capillary alginate hydrogels after spinal cord injury. Acta Biomaterialia 2017;60:167–180.
5. Pang M, Shu T, Chen RQ, Liu C, He L, Yang Y, Bardeesi ASA, Lin CK, Zhang LM, Wang X, Liu B, Rong LM. Neural precursor cells generated from Induced pluripotent stem cells with gelatin sponge-electrospun PLGA/PEG nanofibers for spinal cord injury repair. Int J Clin Exp Med 2016;9:17985–17994.
6. Yu SK, Yao SL, Wen YJ, Wang Y, Wang H, Xu QY. Angiogenic microspheres promote neural regeneration and motor function recovery after spinal cord injury in rats. Sci Rep 2016;6:
7. Hou L, Shan XN, Hao LS, Feng QH, Zhang ZZ. Copper sulfide nanoparticle-based localized drug delivery system as an effective

cancer synergistic treatment and theranostic platform. Acta Biomaterialia 2017;54:307–320.
8. Silver J, Miller JH. Regeneration beyond the glial scar. Nat Rev Neurosci 2004;5:146–156.
9. Schwab ME. Repairing the injured spinal cord. Science 2002;295: 1029–1031.
10. Snider WD. Functions of the neurotrophins during nervous system development: What the knockouts are teaching us. Cell 1994; 77:627–638.
11. Zeng X, Qiu X-C, Ma Y-H, Duan J-J, Chen Y-F, Gu H-Y, Wang J-M, Ling E-A, Wu J-L, Wu W, Zeng Y-S. Integration of donor mesenchymal stem cell-derived neuron-like cells into host neural network after rat spinal cord transection. Biomaterials 2015;53:184–201.
12. Li G, Che M-T, Zhang K, Qin L-N, Zhang Y-T, Chen R-Q, Rong L-M, Liu S, Ding Y, Shen H-Y, Long S-M, Wu J-L, Ling E-A, Zeng Y-S. Graft of the NT-3 persistent delivery gelatin sponge scaffold promotes axon regeneration, attenuates inflammation, and induces cell migration in rat and canine with spinal cord injury. Biomaterials 2016;83:233–248.
13. Radojicic M, Reier PJ, Steward O, Keirstead HS. Septations in chronic spinal cord injury cavities contain axons. Exp Neurol 2005;196:339–341.
14. Cregg JM, DePaul MA, Filous AR, Lang BT, Tran A, Silver J. Functional regeneration beyond the glial scar. Exp Neurol 2014;253: 197–207.
15. Impellizzeri D, Cordaro M, Bruschetta G, Siracusa R, Crupi R, Esposito E, Cuzzocrea S. *N*-palmitoylethanolamine-oxazoline as a new therapeutic strategy to control neuroinflammation: Neuroprotective effects in experimental models of spinal cord and brain injury. J Neurotrauma 2017;34:2609–2623.
16. Simonen M, Pedersen V, Weinmann O, Schnell L, Buss A, Ledermann B, Christ F, Sansig G, van der Putten H, Schwab ME. Systemic deletion of the myelin-associated outgrowth inhibitor Nogo-A improves regenerative and plastic responses after spinal cord injury. Neuron 2003;38:201–211.
17. Oudega M. Molecular and cellular mechanisms underlying the role of blood vessels in spinal cord injury and repair. Cell Tissue Res 2012;349:269–288.
18. Ye J, Ma M, Xie Z, Wang P, Tang Y, Huang L, Chen K, Gao L, Wu Y, Shen H, Zeng Y. Evaluation of the neural function of nonhuman primates with spinal cord injury using an evoked potential-based scoring system. Sci Rep 2016;6:33243.
19. Han S, Wang B, Jin W, Xiao Z, Li X, Ding W, Kapur M, Chen B, Yuan B, Zhu T, Wang H, Wang J, Dong Q, Liang W, Dai J. The linear-ordered collagen scaffold-BDNF complex significantly promotes functional recovery after completely transected spinal cord injury in canine. Biomaterials 2015;41:89–96.
20. McMahill BG, Spriet M, Sisó S, Manzer MD, Mitchell G, McGee J, Garcia TC, Borjesson DL, Sieber-Blum M, Nolta JA, Sturges BK. Feasibility study of canine epidermal neural crest stem cell transplantation in the spinal cords of dogs. Stem Cells Transl Med 2015;4:1173–1186.
21. Olby NJ, De Risio L, Munana KR, Wosar MA, Skeen TM, Sharp NJ, Keene BW. Development of a functional scoring system in dogs with acute spinal cord injuries. Am J Vet Res 2001;62:1624–1628.
22. Li X, Zhao Y, Cheng S, Han S, Shu M, Chen B, Chen X, Tang F, Wang N, Tu Y, Wang B, Xiao Z, Zhang S, Dai J. Cetuximab modified collagen scaffold directs neurogenesis of injury-activated endogenous neural stem cells for acute spinal cord injury repair. Biomaterials 2017;137:73–86.
23. Abbink P, Larocca RA, De La Barrera RA, Bricault CA, Moseley ET, Boyd M, Kirilova M, Li Z, Nganga D, Nanayakkara O, Nityanandam R, Mercado NB, Borducchi EN, Agarwal A, Brinkman AL, Cabral C, Chandrashekar A, Giglio PB, Jetton D, Jimenez J, Lee BC, Mojta S, Molloy K, Shetty M, Neubauer GH, Stephenson KE, Peron JPS, Zanotto P. M d A, Misamore J, Finneyfrock B, Lewis MG, Alter G, Modjarrad K, Jarman RG, Eckels KH, Michael NL, Thomas SJ, Barouch DH. Protective efficacy of multiple vaccine platforms against Zika virus challenge in rhesus monkeys. Science 2016;353:1129–1132.
24. Weishaupt N, Silasi G, Colbourne F, Fouad K. Secondary damage in the spinal cord after motor cortex injury in rats. J Neurotrauma 2010;27:1387–1397.
25. Miller AD, Westmoreland SV, Evangelous NR, Graham A, Sledge J, Nesathurai S. Acute traumatic spinal cord injury induces glial activation in the cynomolgus macaque (Macaca fascicularis). J Med Primatol 2012;41:202–209.
26. Tian DS, Xie MJ, Yu ZY, Zhang Q, Wang YH, Chen B, Chen C, Wang W. Cell cycle inhibition attenuates microglia induced inflammatory response and alleviates neuronal cell death after spinal cord injury in rats. Brain Res 2007;1135:177–185.
27. de Rivero Vaccari JP, Dietrich WD, Keane RW. Therapeutics targeting the inflammasome after central nervous system injury. Transl Res 2016;167:35–45.
28. DiSabato DJ, Quan N, Godbout JP. Neuroinflammation: the devil is in the details. J Neurochem 2016;139:136–153.
29. Sloma EA, Creneti CT, Erb HN, Miller AD. Characterization of inflammatory changes associated with canine oligodendroglioma. J Comp Pathol 2015;153:92–100.
30. Hwang IK, Lee CH, Li H, Yoo KY, Choi JH, Kim DW, Kim DW, Suh HW, Won MH. Comparison of ionized calcium-binding adapter molecule 1 immunoreactivity of the hippocampal dentate gyrus and CA1 region in adult and aged dogs. Neurochem Res 2008;33: 1309–1315.
31. Guo XJ, Tian XS, Ruan Z, Chen YT, Wu L, Gong Q, Wang W, Zhang HY. Dysregulation of neurotrophic and inflammatory systems accompanied by decreased CREB signaling in ischemic rat retina. Exp Eye Res 2014;125:156–163.
32. Kalinowska-Łyszczarz A, Pawlak MA, Michalak S, Paprzycki W, Losy J. Immune cell NT-3 expression is associated with brain atrophy in multiple sclerosis patients. J Neuroimmunol 2011;240–241:109–113.
33. Boyce VS, Tumolo M, Fischer I, Murray M, Lemay MA. Neurotrophic factors promote and enhance locomotor recovery in untrained spinalized cats. J Neurophysiol 2007;98:1988–1996.
34. Elliott Donaghue I, Tator CH, Shoichet MS. Sustained delivery of bioactive neurotrophin-3 to the injured spinal cord. Biomater Sci 2015;3:65–72.
35. Vavrek R, Girgis J, Tetzlaff W, Hiebert GW, Fouad K. BDNF promotes connections of corticospinal neurons onto spared descending interneurons in spinal cord injured rats. Brain 2006;129:1534–1545.
36. Lynskey JV, Sandhu FA, Dai HN, McAtee M, Slotkin JR, MacArthur L, Bregman BS. Delayed intervention with transplants and neurotrophic factors supports recovery of forelimb function after cervical spinal cord injury in adult rats. J Neurotrauma 2006; 23:617–634.
37. Lu P, Jones LL, Tuszynski MH. Axon regeneration through scars and into sites of chronic spinal cord injury. Exp Neurol 2007;203:8–21.
38. Zhang K, Liu Z, Li G, Lai BQ, Qin LN, Ding Y, Ruan JW, Zhang SX, Zeng YS. Electro-acupuncture promotes the survival and differentiation of transplanted bone marrow mesenchymal stem cells pre-induced with neurotrophin-3 and retinoic acid in gelatin sponge scaffold after rat spinal cord transection. Stem Cell Rev 2014;10:612–625.
39. Chen J, Qi JG, Zhang W, Zhou X, Meng QS, Zhang WM, Wang XY, Wang TH. Electro-acupuncture induced NGF, BDNF and NT-3 expression in spared L6 dorsal root ganglion in cats subjected to removal of adjacent ganglia. Neurosci Res 2007;59:399–405.
40. Lai BQ, Wang JM, Ling EA, Wu JL, Zeng YS. Graft of a tissue-engineered neural scaffold serves as a promising strategy to restore myelination after rat spinal cord transection. Stem Cells Dev 2014;23:910–921.
41. Mi S, Hu B, Hahm K, Luo Y, Kam Hui ES, Yuan Q, Wong WM, Wang L, Su H, Chu T-H, Guo J, Zhang W, So K-F, Pepinsky B, Shao Z, Graff C, Garber E, Jung V, Wu EX, Wu W. LINGO-1 antagonist promotes spinal cord remyelination and axonal integrity in MOG-induced experimental autoimmune encephalomyelitis. Nat Med 2007;13:1228–1233.
42. Smith PM, Jeffery ND. Histological and ultrastructural analysis of white matter damage after naturally-occurring spinal cord injury. Brain Pathol 2006;16:99–109.
43. Takeo C, Nakamura S, Tanaka T, Uchida D, Noguchi Y, Nagao T, Saito Y, Tatsuno I. Rat cerebral endothelial cells express trk C and are regulated by neurotrophin-3. Biochem Biophys Res Commun 2003;305:400–406.

44. Valenzuela DM, Maisonpierre PC, Glass DJ, Rojas E, Nunez L, Kong Y, Gies DR, Stitt TN, Ip NY, Yancopoulos GD. Alternative forms of rat TrkC with different functional capabilities. Neuron 1993;10:963–974.
45. Chen YF, Zeng X, Zhang K, Lai BQ, Ling EA, Zeng YS. Neurotrophin-3 stimulates migration of mesenchymal stem cells overexpressing TrkC. Curr Med Chem 2013;20:3022–3033.
46. Schaar KL, Brenneman MM, Savitz SI. Functional assessments in the rodent stroke model. Exp Transl Stroke Med 2010;2:13.
47. Basso DM, Beattie MS, Bresnahan JC. A sensitive and reliable locomotor rating scale for open field testing in rats. J Neurotrauma 1995;12:1–21.
48. Capogrosso M, Milekovic T, Borton D, Wagner F, Moraud EM, Mignardot J-B, Buse N, Gandar J, Barraud Q, Xing D, Rey E, Duis S, Jianzhong Y, Ko WKD, Li Q, Detemple P, Denison T, Micera S, Bezard E, Bloch J, Courtine G. A brain-spine interface alleviating gait deficits after spinal cord injury in primates. Nature 2016;539:284–288.
49. Bunday KL, Perez MA. Impaired crossed facilitation of the corticospinal pathway after cervical spinal cord injury. J Neurophysiol 2012;107:2901–2911.
50. Bhagat S, Durst A, Grover H, Blake J, Lutchman L, Rai AS, Crawford R. An evaluation of multimodal spinal cord monitoring in scoliosis surgery: a single centre experience of 354 operations. Eur Spine J 2015;24:1399–1407.
51. Houweling DA, Lankhorst AJ, Gispen WH, Bar PR, Joosten EA. Collagen containing neurotrophin-3 (NT-3) attracts regrowing injured corticospinal axons in the adult rat spinal cord and promotes partial functional recovery. Exp Neurol 1998;153:49–59.
52. Grill R, Murai K, Blesch A, Gage FH, Tuszynski MH. Cellular delivery of neurotrophin-3 promotes corticospinal axonal growth and partial functional recovery after spinal cord injury. J Neurosci 1997;17:5560–5572.
53. Lapointe NP, Ung RV, Guertin PA. Plasticity in sublesionally located neurons following spinal cord injury. J Neurophysiol 2007;98:2497–2500.
54. Zhang YT, Jin H, Wang JH, Wen LY, Yang Y, Ruan JW, Zhang SX, Ling EA, Ding Y, Zeng YS. Tail nerve electrical stimulation and electro-acupuncture can protect spinal motor neurons and alleviate muscle atrophy after spinal cord transection in rats. Neural Plast 2017;2017:7351238.
55. Hamby ME, Sofroniew MV. Reactive astrocytes as therapeutic targets for CNS disorders. Neurotherapeutics 2010;7:494–506.
56. Sofroniew MV. Molecular dissection of reactive astrogliosis and glial scar formation. Trends Neurosci 2009;32:638–647.
57. Hwang IK, Choi JH, Li H, Yoo K-Y, Kim DW, Lee CH, Yi SS, Seong JK, Lee IS, Yoon YS, Won M-H. Changes in glial fibrillary acidic protein immunoreactivity in the dentate gyrus and hippocampus proper of adult and aged dogs. J Vet Med Sci 2008;70:965–969.
58. Goldshmit Y, Bourne J. Upregulation of EphA4 on astrocytes potentially mediates astrocytic gliosis after cortical lesion in the marmoset monkey. J Neurotrauma 2010;27:1321–1332.